Nucleotide-induced conformational transitions in the CBS domain protein MJ0729 of *Methanocaldococcus jannaschii*

Luis Alfonso Martínez-Cruz[1,6], José Antonio Encinar[2], Paz Sevilla[3,4], Iker Oyenarte[1], Inmaculada Gómez-García[1], David Aguado-Llera[2], Francisco García-Blanco[3], Javier Gómez[2] and José L.Neira[2,5,6]

[1]Unidad de Biología Estructural, CIC bioGUNE, Parque Tecnológico de Bizkaia, 48160 Derio (Vizcaya), Spain, [2]Instituto de Biología Molecular y Celular, Universidad Miguel Hernández, 03202 Elche (Alicante), Spain, [3]Departamento de Química Física II, Facultad de Farmacia, Universidad Complutense de Madrid, 28040 Madrid, Spain, [4]Instituto de Estructura de la Materia, CSIC, 28006 Madrid, Spain and [5]Instituto de Biocomputación y Física de los sistemas complejos, 50009 Zaragoza, Spain

[6]To whom correspondence should be addressed.
E-mail: amartinez@cicbiogune.es (L.A.), jlneira@umh.es (J.L.N.)

Nucleotide-binding cystathionine β-synthase (CBS) domains function as regulatory motifs in several proteins distributed through all kingdoms of life. This function has been proposed based on their affinity for adenosyl-derivatives, although the exact binding mechanisms remain largely unknown. The question of how CBS domains exactly work is relevant because in humans, several genetic diseases have been associated with mutations in those motifs. In this work, we describe the adenosyl-ligand (AMP, ATP, NADP and SAM) properties of the wild-type CBS domain protein MJ0729 from *Methanocaldococcus jannaschii* by using a combination of spectroscopic techniques (fluorescence, FTIR and FRET). The fluorescence results show that binding to AMP and ATP occurs with an apparent dissociation constant of ∼10 μM, and interestingly enough, binding induces protein conformational changes, as shown by FTIR. On the other hand, fluorescence spectra (FRET and steady-state) did not change upon addition of NADP and SAM to MJ0729, suggesting that tryptophan and/or tyrosine residues were not involved in the recognition of those ligands; however, there were changes in the secondary structure of the protein upon addition of NADP and SAM, as shown by FTIR (thus, indicating binding to the nucleotide). Taken together, these results suggest that: (i) the adenosyl ligands bind to MJ0729 in different ways, and (ii) there are changes in the protein secondary structure upon binding of the nucleotides.

Keywords: binding/CBS domain/fluorescence/FTIR/FRET

Introduction

Cystathionine beta-synthase (CBS) domains are 60-residue-long motifs, usually associated in tandems (Bateman, 1997; Zhang *et al.*, 1999), which have been found in several cytosolic and membrane-associated enzymes, and in channels from all species studied to date (Bateman, 1997). They were originally found in cystathionine beta-synthase, after which they were named, and their structure was first described in the inosine monophosphate dehydrogenase (IMPDH) (Zhang *et al.*, 1999). The CBS domains are considered as energy-sensing modules which bind adenosine ligands with different affinities (Scott *et al.*, 2004), although their exact functions are not known. For instance, CBS domains are involved in gating of the osmoregulatory proteins (Biemans-Oldehinkel *et al.*, 2006), in transport and binding of Mg^{2+} (Ishitani *et al.*, 2008), in modulation of intracellular trafficking of chloride channels (Carr *et al.*, 2003), in nitrate transport (De Angeli *et al.*, 2009) and as 'internal inhibitors' of the pyrophosphatase activity (Jämsen *et al.*, 2010; Tuominen *et al.*, 2010). The CBS motifs share common structural properties, either isolated or as domains of larger proteins, despite their low degree of sequence similarity. In fact, several crystal structures have been solved (Lucas *et al.* 2010, and references therein; Tuominen *et al.*, 2010) and all of them show oligomeric folds with a three-stranded β-sheet and two α-helices packed according to a β1-α1-β2-β3-α2 topology within each CBS domain. Furthermore, in most of the structures solved, the CBS domains occur in tandem pairs, forming a so-called CBS pair or Bateman module (Bateman, 1997), in which both CBS subunits are related by a pseudo-two-fold symmetry axis running parallel to the central β-sheet. Those structures show head-to-head or head-to-tail associations of the Bateman modules, thus yielding a total of four CBS domains per structural module (the so-called CBS modules) (Mahmood *et al.*, 2009). However, the adenosyl-ligand affinity varies widely among the different proteins, the stoichiometry of the binding reaction is not known in some domains (Scott *et al.*, 2004) and we do not know whether for the same CBS domain the mode of adenosine-ligand binding changes among the different nucleotides assayed. Furthermore, a few of the solved structures show conformational rearrangement upon ligand binding (Lucas *et al.*, 2010; Tuominen *et al.*, 2010), which can be large in some motifs (Hattori *et al.*, 2007; Ishitani *et al.*, 2008; Tuominen *et al.*, 2010), and we do not know whether this behavior is a general effect.

In humans, several genetic diseases have been associated with mutations in the CBS sequence. For instance, mutations

in chloride channels cause, among others conditions, hyper-calciuric nephrolitiasis; IMPDH mutations cause retinitis pigmentosa and mutations in the γ2-subunit of the AMP-activated protein kinase (AMPK) causes cardiac conductance problems (Kemp, 2004, and references therein). Interestingly enough, most of these disease mutations alter the affinity of CBS domains for adenosine ligands (Scott *et al.*, 2004). Thus, CBS domains can be considered as promising targets for the rational design of new drugs, and understanding how they recognize adenosine derivatives or other biomolecules could help in the drug design.

CBS motifs are abundant in archaea, although scarce information about their function has been reported. Therefore, organisms such as the hyperthermophile *Methanocaldococcus jannaschii* offer excellent models for the characterization of the CBS adenosyl-ligand binding properties (Klenk *et al.*, 1997). The genome of *M.jannaschii* encodes 15 CBS domain proteins (www.tigr.org), which differ significantly in their composition, and probably in their abilities to bind ligands. We recently expressed and isolated the protein MJ0729 from this organism (Fernández-Millán *et al.*, 2008). The open reading frame of the gene MJ0729 (UniProtKB/Swiss-Prot entry Q58139) encodes a polypeptide chain of 124 amino acids with a molecular mass of 14.303 kDa. Its sequence is formed by a CBS domain pair comprising residues 13–60 (the CBS1 domain) and residues 73–122 (the CBS2 domain) (http://smart.embl-heidelberg.de/). Although MJ0729 is currently annotated as an uncharacterized hypothetical protein, it appears close to the genes encoding an iron-sulfur flavoprotein (MJ0731), very similar to a homologue found in *Archaeoglobus fulgidus* (Zhao *et al.*, 2001).

We have previously characterized some biophysical features of MJ0729 (Martínez-Cruz *et al.*, 2009). The protein is an oligomeric highly stable species, whose self-associated properties are pH-dependent. Moreover, the merohedrally twinned trigonal crystals obtained at pH 4.5 show that the protein adopts a disk-like shaped tetrameric fold, with a non-conventional arrangement of the Bateman domains, with dimensions of $65 \times 65 \times 38$ Å (Fernández-Millán *et al.*, 2008; Martínez-Cruz *et al.*, 2009); the merohedral twinning is a special case of crystallographic twinning where the lattices of twin (different) domains (in a single crystal) overlap in three dimensions. An effect of this type of twinning is superimposable lattices, when the rotational symmetry of the lattice exceeds the rotational symmetry of the space group. Both the fold and the dimensions of MJ0729 are different from those found in related proteins (see, for instance, Tuominen *et al.*, 2010), affecting the shape of the ligand binding cavity, and, potentially, its binding capabilities. In this work, we examined the adenine nucleotide affinities of MJ0729 by using several spectroscopic techniques (namely, FTIR, FRET and fluorescence). Our results indicate that (i) nucleotides induced conformational changes in the protein upon binding, and (ii) the apparent affinity of MJ0729 to ATP and AMP is close to 10 μM, as determined by steady-state fluorescence.

Experimental procedures

Materials

Standard suppliers were used for all chemicals. Water was deionized and purified on a Millipore system.

Protein purification

Protein was purified as described (Fernández-Millán *et al.*, 2008). Protein concentrations were calculated from the absorbance of stock solutions measured at 280 nm, using the extinction coefficients of model compounds (Gill and von Hippel, 1989). Protein purities were confirmed by MALDI-TOF and SDS–PAGE.

Steady-state fluorescence

Fluorescence steady-state measurements were carried out on a Cary Eclipse spectrofluorometer (Varian, USA) interfaced with a Peltier temperature-controlling system. A 1-cm-path-length quartz cell (Hellma) was used. Unless it is stated, all binding experiments were performed at 25°C, 50 mM sodium phosphate buffer, pH 8.0. We carried out the binding experiments with ATP, AMP, NADP and SAM adenosine ligands.

Increasing amounts of the ligand, in the range 0–70 μM, were added to a solution of MJ0729 at a fixed protein concentration, 1 or 2 μM (expressed in monomer units). Fluorescence of the resulting samples was measured after overnight incubation time at 4°C to ensure for equilibration. Experiments were carried out with excitation at 280 and 295 nm, and emission fluorescence was collected between 300 and 400 nm. The excitation and emission slits were 5 nm, and the data pitch interval was 1 nm. The dissociation constant of each complex was calculated by fitting the changes observed in the fluorescence intensity at a particular wavelength versus the concentration of the added ligand ([ligand]) to:

$$F_{\text{meas}} = F - \left(\frac{\Delta F_{\text{max}}[\text{ligand}]}{[\text{ligand}] + K_{\text{D}}} \right), \qquad (1)$$

where F_{meas} is the measured fluorescence intensity after subtraction of the blank, ΔF_{max} the change in the fluorescence measured at saturating ligand concentrations, F the fluorescence intensity when no ligand has been added and K_{D} the dissociation constant. We determined the stoichiometry of the reaction, as described by Otzen *et al.* (2005). Inner-filter effects at 280 and 295 nm were corrected for the absorbance of the corresponding ligand (Birdsall *et al.*, 1983). Absorbance measurements were carried out in a Shidmazu UV-1601 ultraviolet spectrophotometer using a 1-cm-path-length cell (Hellma). Typically, every fluorescence titration was repeated three times with freshly prepared samples.

We also carried out binding measurements at pH 5.0, where MJ0729 is mainly a tetrameric species (Martínez-Cruz *et al.*, 2009). None of the ligands modified the fluorescence signal of isolated MJ0729, suggesting that there was no binding at this pH (data not shown).

Fluorescence lifetime measurements

Due to the results obtained with steady-state fluorescence (see Results), we only measured fluorescence lifetimes in the presence of ATP and NADP. The adenosyl derivatives and the protein were prepared in sodium phosphate buffer 50 mM, pH 8.0; the final concentration of protein was 3 μM. The corresponding amounts of ATP or NADP stock solutions

were added to obtain the desired ratio of [ATP]/[protein] or [NADP]/[protein].

Fluorescence lifetimes were measured on an EasyLife V^{TM} lifetime fluorometer (USA) with the stroboscopic technique, using as excitation source a pulsed light of a diode LED of 295 nm and an emission filter of 305 nm to avoid light scattering. By exciting at 295 nm we are only monitoring the fluorescence lifetimes of the sole tryptophan of the protein, at position 49 in the first CBS domain of the MJ0729 monomer. The number of channels used for every scan was 500, and the time of integration (i.e. the time in seconds over which the signal was averaged for every point of each scan) was 1 s. Three scans were averaged in each experiment. Each experiment was repeated two times.

The experimental fluorescence decays ($D(t)$) were fitted to a sum of exponential functions:

$$D(t) = \sum_{i=1}^{n} a_i \exp\left(-\frac{t}{\tau_i}\right), \qquad (2)$$

where τ_i is the corresponding fluorescence lifetime of the species present in solution and a_i the pre-exponential factor for that species. The pre-exponential factors can be interpreted not only in terms of the populations of the corresponding species, but also on terms of the radiative probability constants and the molar extinction coefficients of the respective fluorophores.

We also determined: (i) the mean lifetime, $\bar{\tau}$, as: $\bar{\tau} = \sum_{i=1}^{n} f_i \tau_i$, where the factors, f_i, are defined as: $f_i = a_i \tau_i / \sum_j a_j \tau_j$ and (ii) the amplitude-weighted lifetime, $\langle\tau\rangle$: $\langle\tau\rangle = \sum_{i=1}^{n} a_i \tau_i$.

The fitting procedure of the experimental fluorescence lifetime curves uses an iterative method based on the Marquardt algorithm (Bevington and Robinson, 2003). The temporal width of the excitation pulse, which distorted the observed decay, was taken into account through the instrument response function (IRF), and the IRF was determined experimentally by using a scattered solution of ludox. A new IRF was recorded for every fluorescence lifetime curve measured.

To test the goodness of the fittings, we used two procedures. First, the reduced χ^2 statistic parameter was calculated by measuring the spectral noise at time t and then, we applied a method developed for the stroboscopic optical boxcar to determine the measurement errors (James et al., 1992). And second, we measured the randomness of the residuals by calculating the Durbin–Watson parameter (Durbin and Watson, 1951). This parameter, which must be close to 2 for a satisfactory fit, detects the presence of repeating patterns or periodic signals that have been buried under noise. In our measurements, residuals did not exceed 5%, and the DW parameters in all fittings were always lower than 2.0 (see Results).

FRET measurements

Fluorescence experiments for resonance energy transfer were recorded on a QuantaMaster^{TM} 40 (PTI, Spain) equipped with a high efficiency continuous Xe arc lamp, with an emission wavelength range from 180 to 900 nm. The FRET efficiency, E, was determined by measuring the decrease in the fluorescence intensity of the protein (D) in the presence of the ligand, ATP or NADP (A), according to:

$$E = 1 - \frac{F}{F_0}, \qquad (3)$$

where F_0 and F are the maximum of the fluorescence emission relative intensity of the protein in the absence or in the presence of ligand (for a final rate [ligand]/[protein] = 1), respectively. The distance between D and A, named R_{D-A}, is calculated from:

$$R_{D-A} = \left(\frac{1}{E} - 1\right)^{1/6} R_0, \qquad (4)$$

where R_0, the so-called Förster critical radius, is the donor–acceptor distance corresponding to an energy transfer efficiency of 50%.

Finally, the FRET rate constant, k_{ET}, was calculated according to:

$$k_{ET} = \frac{1}{\tau}\left(\frac{R_0}{R_{D-A}}\right)^6, \qquad (5)$$

where τ is the protein fluorescence lifetime.

The value of R_0 can be calculated using the equation:

$$R_0 = 0.2180 \left(\kappa^2 \Phi_D n^{-4} J_{D-A}\right)^{1/6}, \qquad (6)$$

where $\kappa^2 = 0.66$ is the orientation factor, $\Phi_D = 0.15$ the quantum yield of the tryptophan, $n = 1.33$ the refraction index of the medium and J_{D-A} the spectral overlap integral between the excitation spectrum of the acceptor moiety and the emission spectrum of the donor. The overlap integral was calculated using: $J_{D-A} = C \int_0^\infty I_D(\lambda) E_A(\lambda) \lambda^4 \, d\lambda$, where I_D is the emission spectrum of the donor, E_A the excitation spectrum of the acceptor and C the normalization factor defined as: $C = \varepsilon(\lambda_{max})/E_A(\lambda_{max}) \int_0^\infty I_D(\lambda) \, d\lambda$. The $\varepsilon(\lambda_{max})$ is the molar extinction coefficient of the acceptor at the excitation wavelength. All the integrals were calculated with the FeliX software from Photon Technology International.

Fourier transform infrared spectroscopy

Infrared spectra were recorded in triplicate (600 spectral scans) in a Bruker IF66s instrument (Germany) equipped with a DTGS detector.

(a) Steady state measurements. For infrared Amide I′ band recordings, aliquots of 400 µg of protein in 10 mM HEPES were washed twice with 2 ml of a solution containing 10 mM MOPS, 10 mM CAPS, 10 mM potassium acetate, 100 mM KCl, in the presence or in the absence of 3 mM of the adenosyl-ligands, namely NADP, ATP, SAM and AMP. Sample volume was reduced to about 20 µl by filtration on Vivaspin concentrators (5.000 MW cut-off, Vivascience). The final pHs of the samples were pH 5.0 or 8.0. The concentrated samples were dehydrated in a speedvac Savant rotary evaporator and resuspended in 20 µl of D_2O to prevent the interference of H_2O infrared absorbance (1645 cm^{-1}); thus the protein concentration was 1.3 mM. For the samples in the presence of adenosyl-derivatives, the final concentrations of the ligands were 3 mM (that is, the ratio protein/adenosyl derivative was 1:3). The resulting samples

were placed in a liquid demountable cell equipped with CaF_2 windows and 50 µm thick Mylar spacers and maintained at room temperature for approximately 7 h to reach equilibrium. The buffer contribution was subtracted from the individual spectra, and spectral noise was reduced as described (Echabe *et al.*, 1997).

(b) H/D exchange measurements. Exchange time was started at the moment of the D_2O addition. Spectra were collected at 1 and 10 min, and successively at 9 min intervals for a period of 6 h at 20°C, with the experimental set described above. For initial spectra at 1 min, 10 scans at $2 \, cm^{-1}$ spectral resolution were collected and digitally averaged. For all successive time points, 50 scans were collected (Li *et al.*, 2002). Spectra of buffer blanks in D_2O were collected with the same cell setup and similar time intervals as data when the protein was present; the blank spectra were digitally subtracted from the sample spectra. The Amide II band, with a maximum about $1547 \, cm^{-1}$ and which is ascribed to the N–H bending vibrations of peptide bonds, was used to analyze protein dynamics.

In proteins, the N–H in H_2O is exchanged into N–D in D_2O, and the absorption peak at $1547 \, cm^{-1}$ is decreased, while the N–D bending vibration at about $1450 \, cm^{-1}$ increases their absorption at this frequency (Li *et al.*, 2002). Thus, using a baseline between 1950 and $1750 \, cm^{-1}$, we followed the decrease in the N–H absorption peak to monitor the H/D exchange kinetics. To improve the accuracy in determining the amount of proton exchange, the maximum intensity of the Amide I′ band at 1 min after D_2O exposure, F_{r0}, was used to normalize the absorbance of Amide II band at $t = 1$. The fraction of the remaining amide protons, F_r, is expressed as:

$$F_r = \frac{A_D}{A_H},$$

where A_D and A_H are the normalized maximum intensities of the Amide II in D_2O and H_2O, respectively (Li *et al.*, 2002). Spectra in H_2O were obtained by placing 2 µl of a protein stock at 20 mg/ml, or alternatively, buffer into the chamber with a 6 µm path-length. Values of $A_H = 0.810 \pm 0.059$ (pH 5.0) and 0.684 ± 0.074 (pH 8.0) were obtained for all the samples measured. A two-exponential model was used to describe the decay of the intensity of the amide protons by using the equation:

$$F_r = A_1 \exp(-k_{HX,1})t + A_2 \exp(-k_{HX,2})t + A_3, \quad (7)$$

where A_1, A_2 and A_3 are the fraction of the fast, slow and non-exchanged amide protons under our conditions, and $k_{HX,1}$ and $k_{HX,2}$ are the apparent exchange rate constants for the fast and slow amide protons (Hvidt and Nielsen, 1966; Tatulian *et al.*, 1998; Li *et al.*, 2002; Ferraro *et al.*, 2004).

(c) Band fitting analysis of the steady-state spectra. Protein secondary structure, either in the presence or in the absence of the ligands, was estimated from the FTIR spectra by decomposition of the Amide I′ band into its spectral components (Arrondo *et al.*, 1994; Encinar *et al.*, 2001). Spectra smoothing was carried out by applying the maximum entropy method, assuming that noise and band shape follow a normal distribution. The minimum bandwidth was set to $12 \, cm^{-1}$. The signal-to-noise ratio of the processed spectra

was better than 10 000:1. Derivation of infra-red spectra was performed using a power of 3, breakpoint of 0.3; Fourier self-deconvolution was performed using a Lorenztian bandwidth of $18 \, cm^{-1}$ and a resolution enhancement factor of 2.0.

Results

The CBS domain protein MJ0729 binds adenosine derivatives with micromolar affinity

We explored the binding of adenosyl ligands to MJ0729 by using four different approaches: FTIR, steady-state fluorescence, fluorescence lifetimes and FRET techniques.

The use of the intrinsic fluorescence takes advantage of the fact that the monomer of MJ0729 has a sole tryptophan at position 49, in the first CBS domain, and five tyrosines, two in the first CBS domain (Tyr31 and Tyr37), and three in the second (Tyr99, Tyr120 and Tyr121). Titration curves were acquired for ATP and AMP by excitation at 280 and 295 nm; we observed that, within the error of the measurements (Fig. 1), binding profiles were described by a single-site binding model (hyperbolic curve), with K_D values in the low micromolar range: 21 ± 8 µM for AMP and 7 ± 2 µM for ATP. These data suggest that the tryptophan environment is modified by ligand binding. Interestingly enough, the plots aimed to determine the stoichiometry of adenosyl-ligand:protein (Otzen *et al.*, 2005) led to the values of 7.5 ± 0.8 for AMP and 1.5 ± 0.5 for ATP (Fig. 1). There are one potential binding site per CBS domain, as a monomer of MJ0729 has two CBS domains in tandem (a Bateman motif), those results would indicate that: (i) ATP fulfill both canonical positions of one monomer or, alternatively, (ii) ATP occupies one canonical site of each monomer in the dimeric species and then the two sites of MJ0729 have different affinity [as has been reported for the AMP binding sites in the CBS domain-containing pyrophospahatase of *Moorella thermoacetica* (Jämsen *et al.*, 2010)]. In AMP, such large stoichiometry (that is, eight molecules of AMP per monomer of MJ0729) would indicate that (i) the two canonical sites per monomer are able to allocate that whole number of AMP moieties (since the AMP is smaller than ATP); or, (ii) alternatively there are other non-canonical binding sites in MJ0729, as it has been reported by X-ray studies of MJ1225, where there are three binding sites in a Bateman motif (instead of the usual two) (Gómez-García *et al.*, 2010), which assuming a dimeric form for the AMP-bound MJ0729 species would lead to a value (six sites) very close to that obtained experimentally (7.5 ± 0.8). To the best of our knowledge, there are not reported such large stoichiometry in other CBS domains, suggesting that the binding mechanism is not the same for both nucleotides in MJ0729.

On the other hand, no changes in the fluorescence intensity of MJ0729 were observed upon addition of NADP or SAM (up to concentrations of 18 µM of ligand for 1 µM of MJ0729). Then, we decided to test adenosyl-ligand binding features of those ligands by using other fluorescence approaches. To that end, we carried out FRET measurements by excitation at 295 nm (and thus, only the single tryptophan of MJ0729 was excited) for two of the adenosyl-ligands which showed different behavior during the steady-state fluorescence measurements: ATP and NADP. We observed
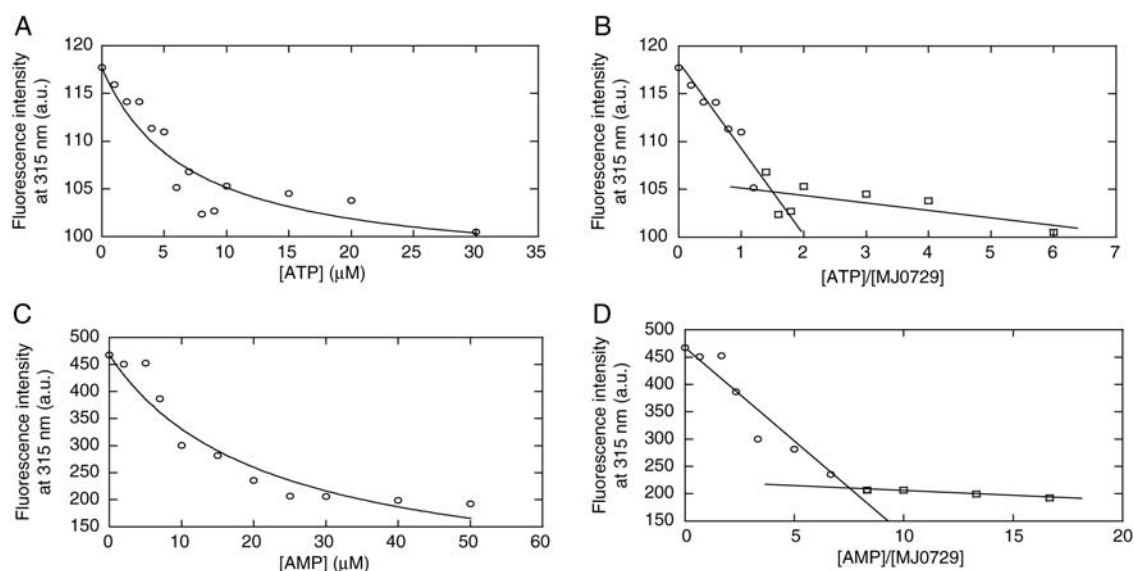
Fig. 1. Fluorescence binding curves. (**A**) Fluorescence titration curves of ATP from the changes in the intensity at 315 nm after excitation at 295 nm (similar titration curves were obtained from excitation at 280 nm and data collection at 315 or 350 nm). The line through the data is the fitting to Equation (1). (**B**) Determination of the stoichiometry for the ATP-MJ0729 binding reaction. (**C**) Fluorescence titration curves of AMP from the changes in the intensity at 315 nm after excitation at 295 nm (similar titration curves were obtained from excitation at 280 nm and data collection at 315 or 350 nm). The line through the data is the fitting to Equation (1). (**D**) Determination of the stoichiometry for the AMP-MJ0729 binding reaction.

Table I. Amplitudes and fluorescence lifetimes for MJ0729 in the presence of growing amounts of NADP or ATP[a]

[Ligand]/ [MJ0279]	ATP								NADP							
	τ_1	a_1	τ_2	a_2	$\bar{\tau}$	$\langle\tau\rangle$	χ^{2b}	DW[c]	τ_1	a_1	τ_2	a_2	$\bar{\tau}$	$\langle\tau\rangle$	χ^{2b}	DW[c]
0[d]	0.19	0.93	5.50	0.07	3.90	0.59	1.18	1.89	0.19	0.93	5.5	0.07	3.90	0.59	1.18	1.89
2	0.79	0.82	4.67	0.18	2.96	1.47	1.16	1.14	0.22	0.95	4.30	0.04	2.13	0.39	1.47	1.15
5	0.62	0.87	4.59	0.13	2.72	1.14	1.21	1.00	0.32	0.93	4.48	0.07	2.44	0.62	1.11	1.29

[a]Measurements were carried out at 25°C. The corresponding τ_is are given in nanoseconds. Measurements at concentrations of [Ligand]/[MJ0729] = 1, 3, 4 and 6 were also carried out, showing similar fluorescence lifetimes and amplitudes to the concentration rates shown here.
[b]The statistical χ^2 parameter for the curve fitting.
[c]The DW statistical parameter (see text for details).
[d]The same values of the fluorescence lifetimes and amplitudes were obtained from two separated measurements. The MJ0729 protein concentration was 3 μM, and the final explored concentration range of ligands was 0–18 μM.

overlapping between the fluorescence emission spectrum of MJ0729 and the absorption spectrum of ATP (at 3 μM equimolar concentrations of both biomolecules). The measurement of the FRET between ATP and MJ0729 at pH 8.0 allowed to determine the $R_0 = 3.67$ nm, $E = 0.035$, $R_{D-A} = 6.37$ nm and $k_{ET} = 8.0 \times 10^6 \, s^{-1}$. Since the limit for detecting energy transfer between two molecules is considered to be 8.0 nm, we can conclude that there is energy transfer between MJ0729 and ATP, but the distance between both molecules is large. On the other hand, there was not overlapping between the fluorescence emission spectrum of MJ0729 and the absorption one of NADP.

The fluorescence lifetimes of Trp49 were adequately described with two exponentials in the isolated protein or in the presence of either ATP or NADP, suggesting two types of rotameric states of the indole moiety (Table I). Every state of the tryptophan of the protein is represented by a discrete lifetime (Ross et al., 1992) (that is, by an exponential decay function), and one of them accounted for the majority of the intensity (that is, it had the larger a_i); the distribution of the

two rotamers and the value of their lifetimes depend, among other factors, on the protein structure and the environment around the tryptophan. The $\langle\tau\rangle$ values obtained for MJ0729 are similar to those observed for other proteins with only one tryptophan in their sequence (see, for instance, Poveda et al., 2007). When the ligand was added, there was a change in the behavior of $\langle\tau\rangle$, and the tendency was different for ATP and NADP. Addition of ATP increased the $\langle\tau\rangle$ of the protein (in the explored ligand concentration range from 0 to 18 μM), indicating that Trp49 was less solvent-exposed, probably due to the binding. However, when NADP was added, the value of $\langle\tau\rangle$ remained unaltered (in the explored ligand concentration range from 0 to 18 μM). These results further support the fact that ATP binds to MJ0729. However, failure to detect any change by any of the fluorescence approaches upon NADP addition could be due to the fact that the environment of Trp49 and its dominant lifetime were not altered upon ligand binding. Alternatively, it could be also thought that the binding affinity of NADP was weaker and we did not explore the appropriate range of ligand

Table II. Secondary structural analysis of MJ0729 (in %) as determined by FTIR at 25°C[a]

MJ0729		MJ0729+NADP		MJ0729+ATP		MJ0729+AMP		MJ0729+SAM	
Band position	Band area ± SD (%)	Band position	Band area ± SD (%)	Band position	Band area ± SD (%)	Band position	Band area ± SD (%)	Band position	Band area ± SD (%)
1687.5	0.1 ± 0.1			1687.9	1.5 ± 0.3	1687.9	1.5 ± 0.1	1687.9	1.1 ± 0.3
1677	11.3 ± 0.2	1680.5	9.2 ± 0.9	1677.6	6.7 ± 0.2	1677.2	8.0 ± 0.3	1677.8	6.6 ± 0.7
1666.7	9.7 ± 0.1	1668.9	4 ± 2	1667.6	10.6 ± 0.7	1666.7	10.6 ± 0.2	1667.8	10.7 ± 0.7
1656.4	21.2 ± 1.0	1656.4	42 ± 3	1656.4	24 ± 2	1656.6	19.2 ± 0.5	1656.4	26 ± 1
1647	25.5 ± 0.8	1646.3	16 ± 1	1647.4	25 ± 1	1647	29.8 ± 0.1	1647.4	24.6 ± 0.9
1636	23.5 ± 0.1	1636.3	23 ± 1	1636.5	24.9 ± 0.5	1635.8	25.2 ± 1.1	1636.3	25.4 ± 0.5
1624.9	8.4 ± 0.5	1625.5	5.5 ± 0.8	1625.3	6.8 ± 0.7	1624.6	5.1 ± 0.1	1624.9	5.3 ± 0.4
1612.4	0.3 ± 0.2	1613.2	0.3 ± 0.1	1613.5	0.5 ± 0.1	1613.2	0.6 ± 0.0	1612.9	0.3 ± 0.1

[a]Band position (cm^{-1}) and percentage area (mean ± SD, $n = 3$) corresponding to the components obtained after curve fitting of the Amide I′ band of MJ0729 in the absence and in the presence of 3 mM of NADP, ATP, AMP and SAM in buffer 10 mM MOPS, 10 mM CAPS, 10 mM potassium acetate (pH 8.0), 100 mM KCl.

concentrations; however, the use of higher ligand concentrations in fluorescence was not possible due to inner-filter effects. Thus, we examined the possible adenosyl-ligand binding to MJ0729 by using a complementary technique.

Binding of the adenosyl derivatives to MJ0729 involves protein conformational changes

The use of the fluorescence allowed us to monitor adenosyl-ligand binding and structural changes around Trp49 and/or tyrosine residues. Attempts to monitor binding and possible protein structural changes by circular dichroism (where the secondary structure is monitored) failed due probably to the small size of the ligands (data not shown). Thus, we decided to use FTIR as a complementary approach to: (i) explore the binding of the adenosyl ligands to the protein, and (ii) elucidate whether binding induced conformational changes in MJ0729.

FTIR is a powerful method for the investigation of secondary and tertiary structures, by following spectroscopic changes of Amide I′ and II (1700–1500 cm^{-1}). The absorbance of the Amide I′ region of protein spectra is mainly due to the stretching vibration of the carbonyl peptide bond, whose frequency is highly sensitive to hydrogen bonding and, thus, to protein secondary structure (Surewicz and Mantsch, 1988). In addition, monitoring the H/D exchange properties of the Amide II′ can give insight into the stability of the protein in the absence or in the presence of ligands.

We investigated the bands of the FTIR spectra at pH 5.0 and pH 8.0 in MJ0729 in the absence and in the presence of ATP, AMP, SAM and NADP. In the absence of ligands, the Amide I′ band of the FTIR spectrum of MJ0729 at both pHs was centered at 1647 cm^{-1}, which is characteristic of the presence of non-ordered conformations. Fourier self-deconvolution and derivation analysis (see Experimental Procedures) exhibited the maxima shown in Table II. These values are similar to those previously observed at pH 7.0 (Martínez-Cruz et al., 2009). The 1612 cm^{-1} component corresponds to tyrosine side-chain vibrations (Fabian and Mantsch, 1995), and the other maxima are assigned to vibration of groups involved in different secondary structural motifs. The bands at 1624 and 1636 cm^{-1} are assigned to inter- and intramolecular (π, 0) β-sheet structure, respectively. The 1646 cm^{-1} band is assigned to random coil. The

1656 cm^{-1} band is assigned to α-helix or disordered structure. The bands at 1666, 1677 and 1687 cm^{-1} bands are due to turns and loops. However, upon ligand addition, the percentages of the secondary structure at pH 8.0 were changed (Table II). The largest differences occurred in the presence of NADP, which was able to increase the α-helical content by approximately 20%. In the presence of ATP and AMP, the percentages of secondary structure remained basically unaltered at pH 8.0, when compared with isolated MJ0729, although slight changes in the population of inter- and intramolecular (π, 0) β-sheet structure were observed, as well as in the turn and loop populations (Table II); on the other hand, the presence of SAM changed slightly the populations of α-helix. It could be thought that the changes observed in the FTIR spectra were due to the presence of the adenosyl-moieties, but adenine and the rest of the bases absorb at 1620 cm^{-1}, where the in-plane vibration of the adenine bases occurs (Banyay et al., 2003). Thus, we conclude that: (i) FTIR results support the binding of the adenosyl-ligands to MJ0729, and (ii) there were changes in the protein secondary structure upon binding, and not only around the tryptophan and tyrosine residues (as monitored by fluorescence). Conversely, we did not observe changes in the percentages of secondary structure, when compared with isolated MJ0729, at pH 5.0 (data not shown).

We further monitored the changes in the secondary and tertiary structures by H/D exchange measurements in the absence or in the presence of nucleotides. The H/D results indicate that at pH 5.0 none of the ligands was bound to MJ0729 (data not shown); in contrast, at pH 8.0, we observed a clear interaction between MJ0729 and some of these adenosine derivatives. At this pH, three groups of nucleotides could be distinguished (Table III): (i) the group formed by SAM, where F_{r0} is similar to that of isolated MJ0729 and the fraction of non-exchanged protons, A_3, is smaller than that of the isolated protein, (ii) AMP, where the F_{r0} is larger than in isolated MJ0729, and A_3 is similar to that of isolated MJ0729, and (iii) NADP and ATP, where their F_{r0}s and A_3 are larger than those of isolated MJ0729. Thus, the FTIR results indicate that: (i) the four ligands bind to MJ0729, and (ii) upon binding, there were changes in the solvent protection of the amide protons, probably due to conformational changes in the protein.

Table III. H–D measurements of MJ0729 in the absence and in the presence of adenosyl ligands[a]

Ligand	F_{r0}[b]	A_1[c]	$k_{HD,1}$ (min^{-1})	A_2[c]	$k_{HD,2}$ (min^{-1})	A_3[c]
Isolated MJ0729	0.75 ± 0.04	0.183 ± 0.007	0.047 ± 0.007	0.13 ± 0.03	0.006 ± 0.01	0.45 ± 0.02
NADP	0.852 ± 0.007	0.032 ± 0.002	0.037 ± 0.008	0.237 ± 0.001	0.002 ± 0.001	0.59 ± 0.01
ATP	0.86 ± 0.03	0.091 ± 0.004	0.032 ± 0.006	0.21 ± 0.01	0.004 ± 0.001	0.56 ± 0.01
SAM	0.764 ± 0.007	0.13 ± 0.01	0.04 ± 0.01	0.290 ± 0.006	0.005 ± 0.002	0.35 ± 0.03
AMP	0.84 ± 0.01	0.18 ± 0.02	0.044 ± 0.007	0.19 ± 0.03	0.005 ± 0.001	0.48 ± 0.05

[a]Measurements were carried out at pH 8 and 25°C.
[b]F_{r0} is the non-exchanged fraction 1 min after D_2O exposure.
[c]A_i are the fractions of amide protons in the ith population that exchange with rate constant $k_{HX,i}$.

Discussion

### Binding of AMP and ATP to the CBS domain MJ0729 protein involves conformational rearrangements

Although the growing number of crystal structures of CBS domain proteins allow us to know with relative certainty the potential location of their binding sites, we still cannot accurately predict the specific ligands that can interact with the protein, and even less how this binding becomes a signal that regulates their biological activity. Furthermore, we do not know whether there are changes in the protein structure upon binding, or whether different nucleotides bound to the same protein, do so in different modes. Much of our inability to make reasonable predictions is due to the small number of structures of CBS domain–ligand complexes known, in contrast with the elevated number of apo-forms currently deposited in the PDB. In all described examples, CBS domains are associated in tandem pairs to form the Bateman domains. Given the available structures, it seems well-established that binding of adenosine derivatives to CBS domains usually requires the presence of two Bateman domains, which in turn associate to form dimers that can be oriented in a head-to-head or a head-to-tail manner. The relative orientation of the Bateman domains determines not only the size of the cavity that accommodates each ligand but also the location of key residues involved in the interaction with small molecules or with metallic ions upon dimerization.

Similarly to other proteins of this family, each of the two CBS domains of the protein MJ0729 consists of a three-stranded β-sheet and two α-helices packed according to the sequence β1-α1-β2-β3-α2 (Martínez-Cruz *et al.*, 2009). The ordering of both subunits in tandem generates two similar-sized cavities which are related by a dyad axis running parallel to the β-sheets. These clefts are analogous to those that have been proven to be the potential binding site for adenosyl groups in ClC-5 and AMPK (Amodeo *et al.*, 2007; Day *et al.*, 2007; Jin *et al.*, 2007; Meyer *et al.*, 2007; Townley and Shapiro, 2007; Xiao *et al.*, 2007). However, one of the main features distinguishing MJ0729 from other CBS domain proteins is that its oligomerization state is pH-dependent. Additionally, the orientation adopted by the Bateman domains in the tetrameric species (observed to be the dominant oligomeric forms at pH 4.5–4.8) differs from that observed in related proteins and can be considered an intermediate between the head-to-head and head-to-tail arrangements (Martínez-Cruz *et al.*, 2009). Such orientation affects the size and the properties of each cavity (see below), which can accommodate potential ligands. Although we have

not been able to obtain high-quality crystals of the dimeric species so far, which is the dominant species between pH 7.0 and 8.0, data from our laboratories indicate that the dimer probably maintains the anomalous orientation of the Bateman domains observed in the tetramer (Martínez-Cruz *et al.*, 2009).

The MJ0729 was bound to AMP and ATP at pH 8.0, but ADP did not show any interaction [as suggested by surface plasmon resonance studies with ADP; conversely, the rest of the ligands described in this work were shown to be bound to MJ0729 by the surface plasmon resonance technique (data not shown)]. The FTIR and steady-state fluorescence showed binding of both ligands to the protein at this pH; furthermore, the FTIR results suggest that the binding affect the structure of the protein. The affinities, as measured by fluorescence, were similar to those observed for other CBS domains for the same adenosyl derivatives (Scott *et al.*, 2004; Jämsen *et al.*, 2010), showing an hyperbolic curve (Fig. 1); however, the dissimilar stoichiometry for both ligands suggest that the mode of binding is different, probably due to the different size of the nucleotide. The steady-state fluorescence results further suggest that the tryptophan is close to (at least to one of them) the AMP (see Results) binding sites and/or the canonical ATP binding site. We can support these experimental findings by having a close look to the three-dimensional structure of a monomer of MJ0729 at pH 4.5 (Fig. 2): Trp49 is close to the proposed binding Site 2, whereas Tyr121 and Tyr37 are close to the proposed binding Site 1. However, it must brought in mind that the positions of the aromatic rings in the solved structure are those observed in one of the monomers of the tetramer at pH 4.5 (Fernández-Millán *et al.*, 2008), and then the surroundings around those fluorescence residues could change as the pH is increased (Martínez-Cruz *et al.*, 2009).

It is important to indicate that binding occurs only in a narrow pH range (pH 7.0 to 8.0), where the dominant dimeric species seems to be dominant (Martínez-Cruz *et al.*, 2009). We carried out steady-state fluorescence, H/D exchange FTIR measurements and steady-state FTIR spectra at pH 5.0 [where the dominant species self-associated species is a tetramer (Martínez-Cruz *et al.*, 2009)]; we did not observe binding for any of the ligands, nor variation in the protein amide exchange rates in the presence of any of the adenosyl-derivatives, when compared to those of the isolated protein at the same pH. We hypothesize that the titration of the phosphate groups of the corresponding ligand (Tinoco *et al.*, 1995), which together with the adenosyl-moiety, are involved in the binding to CBS domains
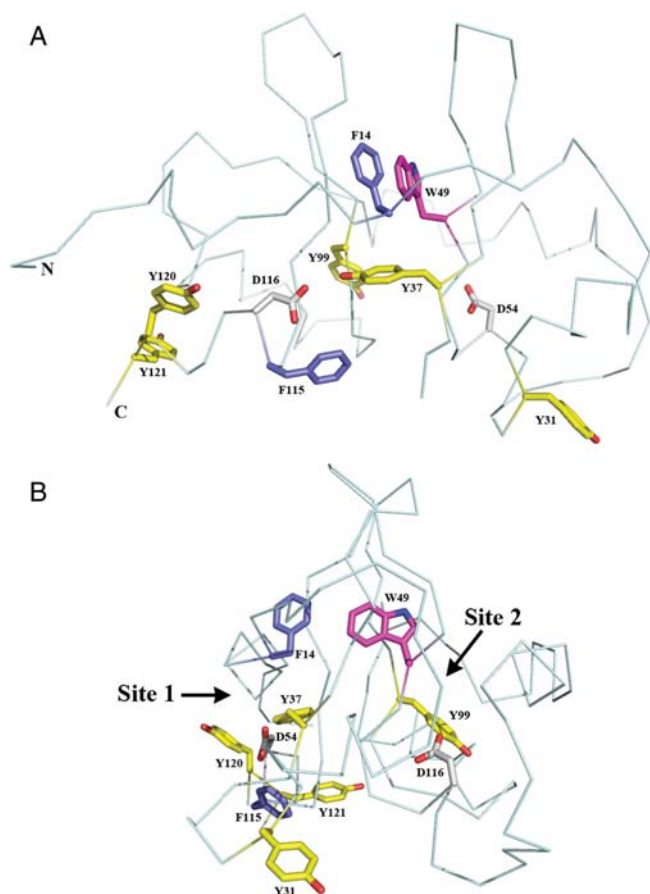
Fig. 2. Crystal structure of the monomer of MJ0729. The Cα main chain of the MJ0729 monomer as determined from the crystal structure of the protein at pH 4.5 (Martínez-Cruz et al., 2009). The side chain of the aromatic residues—two phenylalanines, five tyrosine and one tryptophan residues—are represented with sticks. The picture was done with PyMOL (http://www.pymol.org) (Delano, 2002). The lower part of the figure depicts a rotation of 90 degrees around the vertical pseudo 2-fold axis that relates the two CBS subunits contained within each monomer. The location of the two potential binding sites for adenine nucleotides is indicated. The sites have been numbered following the nomenclature proposed by Kemp et al. (2007).

(Amodeo et al., 2007; Day et al., 2007; Jin et al., 2007; Meyer et al., 2007; Townley and Shapiro, 2007; Xiao et al., 2007), might be also responsible for the lack of binding at this pH.

Binding of SAM and NADP to the CBS domain MJ0729 protein also involve conformational rearrangement, but the Trp49 does not intervene in the affinity reaction

Fluorescence results suggest that the environment of the sole Trp and/or several Tyr did not change upon binding to NADP nor SAM. However, the: (i) FTIR H/D exchange measurements (Table III), and (ii) variations in the populations of secondary structure in the presence of the ligands, as suggested by FTIR deconvolution (Table II), indicate binding. Since the tryptophan and tyrosine residues seem to be close enough to Sites 1 and 2 in the monomer (Fig. 2), we suggest that the structures of the binding-competent species for those ligands must be different to the monomeric structure of MJ0729 reported at pH 4.5 (Martínez-Cruz et al., 2009) and then the fluorescent residues must have been pulled apart from the neighborhood of the canonical

binding sites. We must keep in mind that the FTIR experiments were carried out at high protein concentrations and that MJ0729 has several self-associated species in equilibrium; according to Le Chatelier's principle, the population of self-associated species should increase at high protein concentrations. These other self-associated species able to bind NADP and SAM would scavenge the adenosyl-derivatives from the solution and, then, we could detect a variation in the exchange protection of the overall population of the protein-bound species (probably due to the self-association), and further, we would be able to monitor global changes in the percentage of protein secondary structure (since the structure of those nucleotide-bound protein species should not be completely native-like).

How can these results be related to the biological function of MJ0729? Probably, from a biological point of view and in the absence of as yet unclear function for MJ0729, neither NADP nor SAM is the natural substrate of MJ0729. Interestingly enough, the chloride channel CLC-5 does not show either a large affinity for NADP (Meyer et al., 2007) and the affinity of some mutants of the CBS protein for SAM is also very low (Scott et al., 2004). Thus, it might be the fact that CBS domains are able to bind adenosyl-ligands is the remnant of an ancient more general function of this widely distributed domain, and that is why, in some CBS domains, the adenosyl-ligand affinity is so low. We are carrying out in our laboratories a general 'fishing' approach to detect other biomolecules able to bind to the several CBS domains we are working on.

References

Amodeo,G.A., Rudolph,M.J. and Tong,L. (2007) Nature, **449**, 492–495.

Arrondo,J.L.R., Castresana,J., Valpuesta,J.M. and Goñi,F.M. (1994) *Biochemistry*, **33**, 11650–11655.

Banyay,M., Sarkar,M. and Graslund,A. (2003) *Biophys. Chem.*, **104**, 477–488.

Bateman,A. (1997) *Trends Biochem. Sci.*, **22**, 12–13.

Bevington,P.R. and Robinson,K.D. (2003) *Data reduction and Error Analysis for the Physical Sciences*, 3rd edn. McGraw-Hill, New York.

Biemans-Oldehinkel,E., Mahmood,N. and Poolman,B. (2006) *Proc. Natl Acad. Sci. USA*, **103**, 10624–10629.

Birdsall,B., King,R.W., Wheeler,M.R., Lewis,C.A., Jr., Goode,S., Dunlap,R.B. and Roberts,G.C.K. (1983) *Anal. Biochem.*, **132**, 353–361.

Carr,G., Simmons,N. and Sayer,J. (2003) *Biochem. Biophys. Res. Commun.*, **310**, 600–605.

Day,P., Sharff,A., Parra,L., *et al*. (2007) *Acta Crystallogr. D*, **63**, 587–596.

De Angeli,A., Moran,O., Wege,S., Filleur,S., Ephritikhine,G., Thomine,S., Barbier-Brygoo,H. and Gambale,F. (2009) *J. Biol. Chem.*, **284**, 26526–26532.

DeLano,W.L. (2002). *The PyMOL Molecular Graphics System*. DeLano Scientific, San Carlos, CA.

Durbin,J. and Watson,G.S. (1951) *Biometrika*, **38**, 159–178.

Echabe,I., Encinar,J.A. and Arrondo,J.L.R. (1997) *Biospectroscopy*, **3**, 469–475.

Encinar,J.A., Mallo,G.V., Mizyrycki,C., *et al*. (2001) *J. Biol. Chem.*, **276**, 2742–2751.

Fabian,H. and Mantsch,H.H. (1995) *Biochemistry*, **34**, 13651–13655.

Fernández-Millán,P., Kortazar,D., Lucas,M., *et al*. (2008) *Acta Crystallogr. F*, **64**, 605–609.

Ferraro,D.M., Lazo,N.D. and Robertson,A.D. (2004) *Biochemistry*, **43**, 587–594.

Gill,S.C. and von Hippel,P.H. (1989) *Anal. Biochem.*, **182**, 319–326.

Gómez-García,I., Oyenarte,I. and Martínez-Cruz,L.A. (2010) *J. Mol. Biol.*, **399**, 53–70.

Hattori,M., Tanak,Y., Fukai,S., Ishitani,R. and Nureki,O. (2007) *Nature*, **448**, 1072–1075.

Hvidt,A. and Nielsen,S.O. (1966) *Adv. Prot. Chem.*, **21**, 287–386.

Ishitani,R., Sugita,Y., Dohmae,N., Furuya,N., Hattori,M. and Nureki,O. (2008) *Proc. Natl Acad. Sci. USA*, **105**, 15393–15398.

James,D.R., Siemiarczuk,A. and Ware,W.R. (1992) *Rev. Sci. Instrum.*, **63**, 1710–1716.

Jämsen,J., Baykov,A.A. and Lahti,R. (2010) *Biochemistry*, **49**, 1005–1013.

Jin,X., Townley,R. and Shapiro,L. (2007) *Structure*, **15**, 1285–1295.

Kemp,B.E. (2004) *J. Clin. Invest.*, **113**, 182–184.

Kemp,B.E., Oakhill,J.S. and Scott,J.W. (2007) *Structure*, **15**, 1161–1163.

Klenk,H.P., Clayton,R.A., Tomb,J.F., *et al*. (1997) *Nature*, **390**, 364–370. [Erratum: (1998) Nature, 394, 101].

Li,J., Cheng,X. and Lee,J.C. (2002) *Biochemistry*, **41**, 14771–14778.

Lucas,M., Encinar,J.A., Arribas,E.A., *et al*. (2010) *J. Mol. Biol.*, **396**, 800–820.

Mahmood,N.A., Biemans-Oldehinkel,E. and Poolman,B. (2009) *J. Biol. Chem.*, **284**, 14368–14376.

Martínez-Cruz,L.A., Encinar,J.A., Kortazar,D., *et al*. (2009) *Biochemistry*, **48**, 2760–2776.

Meyer,S., Savaresi,S., Forster,I.C. and Dutzler,R. (2007) *Nat. Struct. Mol. Biol.*, **14**, 60–67. [Erratum: (2007) Nat. Struct. Mol. Biol., 14, 172].

Otzen,D.E., Lundvig,D.M., Wimmer,R., Nielsen,L.H., Pedersen,J.R. and Jensen,P.H. (2005) *Protein Sci.*, **14**, 1396–1409.

Poveda,J.A., Fernández-Ballester,G., Prieto,M. and Neira,J.L. (2007) *Biochemistry*, **46**, 7252–7260.

Ross,J.B., Wyssbrod,H.R., Porter,A.R., Schwartz,G.P., Michaels,C.A. and Laws,W.R. (1992) *Biochemistry*, **31**, 1585–1594.

Scott,J.W., Hawley,H.A., Green,K.A., Anis,M., Stewart,G., Scullion,G.A., Norman,D.G. and Hardie,D.H. (2004) *J. Clin. Invest.*, **113**, 274–284.

Surewicz,W.K. and Mantsch,H.H. (1988) *Biochim. Biophys. Acta*, **952**, 115–130.

Tatulian,S.A., Cortes,D.M. and Perozo,E. (1998) *FEBS Lett.*, **423**, 205–212.

Tinoco,I., Jr., Sauer,K. and Wang,J.C. (1995) *Physical Chemistry: Principles and Applications in the Biological Sciences*, 3rd edn. Prentice Hall, New York.

Townley,R. and Shapiro,L. (2007) *Science*, **315**, 1726–1729.

Tuominen,H., Salminen,A., Oksanen,E., *et al*. (2010) *J. Mol. Biol.*, **398**, 400–413.

Xiao,B., Heath,R., Saiu,P., *et al*. (2007) *Nature*, **449**, 496–500.

Zhang,R., Evans,G., Rotella,F.J., Westbrook,E.M., Beno,D., Huberman,E., Joachimiak,A. and Collart,F.R. (1999) *Biochemistry*, **38**, 4691–4700.

Zhao,T., Cruz,F. and Ferry,J.G. (2001) *J. Bacteriol.*, **183**, 6225–6233.